PHYSICAL REVIEW B VOLUME 34, NUMBER 6 15 SEPTEMBER 1986

Magnetic properties of binary intermetallic Zintl phases of the $B32$ type

Peter C. Schmidt
Institut für Physikalische Chemie, Physikalische Chemie III, Technische Hochschule
Darmstadt, Petersenstrasse 20, D-6100 Darmstadt, West Germany

(Received 24 June 1985; revised manuscript received 23 October 1985)

The magnetic spin susceptibility $\chi^{(\hat{s})}$ and Knight shift $K_s^{(\hat{s})}$ are calculated for the intermetallic $A^{\mathrm{I}a}B^{\mathrm{III}a}$ compounds LiAl, LiGa, LiIn, and NaIn and for the $AB^{\mathrm{I}a}B^{\mathrm{II}b}$ compounds LiZn and LiCd. For the $A^{\mathrm{I}a}B^{\mathrm{III}a}$ compounds, the investigations have been performed for the stoichiometric (ideal) structure as well as for a defect structure with vacancies in the alkali sublattice and substitutionals in the $B^{\mathrm{III}a}$ sublattice. The self-consistent scalar relativistic spin-polarized augmented-plane-wave method is used for these investigations. From the exchange polarization effect one finds that the exchange enhancement of $\chi^{(\hat{s})}$ is in the range of 10% for the $A^{\mathrm{I}a}B^{\mathrm{III}a}$ compounds and of about 30% for the $A^{\mathrm{I}a}B^{\mathrm{II}b}$ compounds. Considering $K_s^{(\hat{s})}$, the first two valence bands give a negative exchange polarization, which is found to be larger than the exchange enhancement effect for the electronic states at the Fermi surface. The calculated spin values $K_s^{(\hat{s})}(A\underline{B})$ show the same trend as the experimental K_s elements for all compounds studied here. For all $A^{\mathrm{I}a}B^{\mathrm{III}a}$ compounds, however, satisfactory results are only obtained for the defect phases. From the comparison of K_s^{theor} and K_s^{expt}, one can conclude that for the Li$B^{\mathrm{III}a}$ phases the number of valence electrons per unit cell should be more than 0.5 to 3.5% smaller than the value for the perfect lattice.

I. INTRODUCTION

Binary intermetallic Zintl phases AB of the $B32$ type are formed by alkali metals $A^{\mathrm{I}a}=$Li and Na with group-IIIa elements $B^{\mathrm{III}a}=$Al, Ga, In, and Tl and elements $B^{\mathrm{II}b}=$Zn and Cd.[1] The physical properties of these compounds suggest that the chemical bonding in these phases is a mixture of metallic, covalent, and ionic contributions.[2] This is also found in theoretical investigations of the electronic structure of $B32$-type Zintl phases.[3-8]

From measurements of the Knight shift K_s it is found that the chemical shifts in the $A^{\mathrm{I}a}B^{\mathrm{III}a}$ phases are distinctly smaller than those in the pure metals, whereas in the $A^{\mathrm{I}a}B^{\mathrm{II}b}$ cases the values for K_s are close to the values in the metals.[9] Such a difference in the physical behavior between the $A^{\mathrm{I}a}B^{\mathrm{II}b}$ and the $A^{\mathrm{I}a}B^{\mathrm{III}a}$ Zintl phases is less marked with respect to the magnetic susceptibility χ.[10,11] The experimental results suggest, however, that the spin contribution to χ is distinctly larger for the $A^{\mathrm{I}a}B^{\mathrm{II}b}$ than for the $A^{\mathrm{I}a}B^{\mathrm{III}a}$ alloys.[10,11] Besides the spin contributions to χ, paramagnetic and diamagnetic orbital contributions are expected to be of the same order of magnitude.[5,9] In the present paper the two spin contributions (direct and exchange polarization) to K_s and χ are gained from spin-polarized self-consistent scalar relativistic band-structure calculations using the augmented-plane-wave method.

From structural investigations of the $A^{\mathrm{I}a}B^{\mathrm{III}a}$ Zintl compounds it is suggested that a defect structure is present in these phases with about 3% vacancies in the alkali sublattice V_A and substitutionals in the $B^{\mathrm{III}a}$ sublattice A_B.[12] Studying the magnetic properties of these phases theoretically the defects can be taken into account in a first approximation by the use of the rigid-band model. In this approach the number of defects influences the number of valence electrons per lattice site and thereby the position of the Fermi level. For the perfect lattice the number of valence electrons per half unit cell N_{VE} is equal to 4 for the $A^{\mathrm{I}a}B^{\mathrm{III}a}$ compounds. In the present paper these phases are called stoichiometric phases. For the defect phases with defects V_A and A_B, N_{VE} is smaller than 4. For LiAl one finds $N_{VE}\approx 3.92$.[12] It is assumed that a similar defect structure is present in all $A^{\mathrm{I}a}B^{\mathrm{III}a}$ Zintl compounds.[12] For LiAl (Ref. 5) and NaTl (Ref. 6), it is found that the calculated Fermi contact contributions to K_s differ distinctly for the cases $N_{VE}=4$ and $N_{VE}<4$. To see whether our theoretical studies support the assumption of the defect structure we have calculated the spin contribution to χ and K_s for both cases, the stoichiometric (ideal) and defect phases $A^{\mathrm{I}a}B^{\mathrm{III}a}$.

The method used for these calculations is described in a previous paper.[6] In the next section the spin contributions to χ and K_s are given. For LiAl, LiZn, and LiCd our results for the direct spin contributions to χ and K_s are compared with data from Asada *et al.*,[5] who obtained the direct contributions by a linear combination of atomic orbitals (LCAO) type method. Finally, in Sec. III the trends in K_s in the series of $B32$-type compounds are discussed.

II. RESULTS

A. Band-structure data

The band structures of the different Zintl phases of the $B32$ type are rather similar.[7,8] The following lattice parameters are used for the present calculations: $a(\mathrm{LiAl})=12.019a_0$, $a(\mathrm{LiZn})=11.733a_0$, $a(\mathrm{LiGa})=11.707a_0$, $a(\mathrm{LiCd})=12.636a_0$; and $a(\mathrm{LiIn})=12.823a_0$. In Fig. 1 the band structure and density of states $n(E)$ are

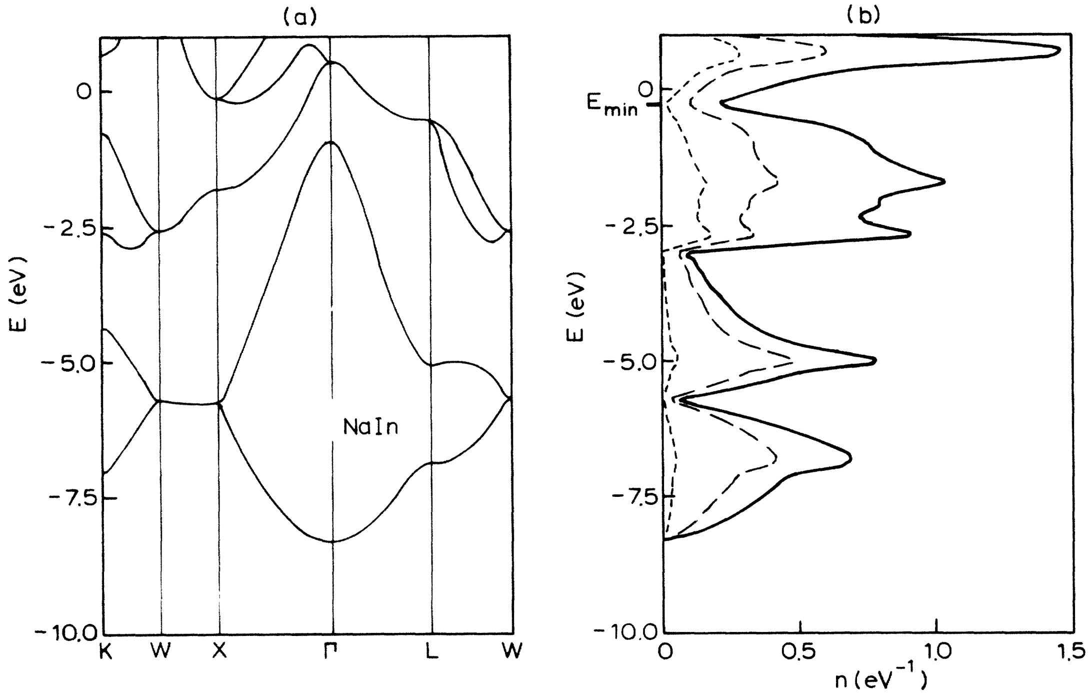

FIG. 1. (a) Band structure of the valence bands of NaIn. The zero of the energy scale is the Fermi energy E_F. (b) Density of states $n(E)$ for the bands shown on the left-hand side. Thick line: total density of states per formula unit NaIn, thick dashed line: partial density of states for the In sphere; thin dashed line: partial density of states for the Na sphere.

displayed for NaIn as an example. The band structures of the other compounds of this type are published elsewhere.$^{4-8}$ For an understanding of the magnetic data a few band-structure properties have to be considered.

For the $A^{\mathrm{Ia}}B^{\mathrm{IIIa}}$ compounds the Fermi energy E_F is in the energy region of the third sharp minimum of the density of states, labeled $E_{\min}$ in Fig. 1. For the stoichiometric $A^{\mathrm{Ia}}B^{\mathrm{IIIa}}$ phases with four valence electrons per half unit cell, $N_{VE}=4$, E_F is larger than $E_{\min}$. Assuming for the defect phases (see Sec. I) a reduction of the N_{VE} of 2%, E_F is lowered by approximately 0.2 eV and $E_F \approx E_{\min}$. Only in the case of NaIn is a slightly larger defect of N_{VE} necessary to lower E_F to $E_{\min}$. In the present paper $E_F \approx E_{\min}$ is taken for the defect phases.

For the stoichiometric $A^{\mathrm{Ia}}B^{\mathrm{IIIa}}$ phases the sheets of the Fermi surface are formed by the second to sixth valence bands, which can be seen for the example LiAl from Table I, where the number of valence electrons is listed bandwise. For the defect phases the fifth and sixth bands are empty.

The density of states at the Fermi surface $n(E_F)$ is also listed in Table I. For the defect $A^{\mathrm{Ia}}B^{\mathrm{IIIa}}$ phases it is found that $n(E_F)$ is smaller by a factor of about 2 compared to the stoichiometric ones, because $E_F(\text{defect}) \approx E_{\min}$. For the $A^{\mathrm{Ia}}B^{\mathrm{IIb}}$ phases, $n(E_F)$ is much larger than $n(E_F, A^{\mathrm{Ia}}B^{\mathrm{IIIa}})$, since $E_F(A^{\mathrm{Ia}}B^{\mathrm{IIb}})$ lies below $E_{\min}$ in the energy range of large values of $n(E)$. This can be seen from Fig. 1 because of the large similarities in the band

TABLE I. Occupation numbers and density of states for LiAl. The bandwise contributions and the total results are listed for (a) the number of electrons per formula unit LiAl N, (b) the difference in the numbers of spin-up and spin-down electrons per formula unit LiAl $\Delta N = N_+ - N_-$, and (c) the density of states at the Fermi surface per Ry and per formula unit LiAl $n(E_F)$. The results are listed for stoichiometric LiAl and for the defect phase LiAl.

	Stoichiometric phase			Defect phase		
	N	ΔN	$n(E_F)$	N	ΔN	$n(E_F)$
First band	1	0	0	1	0	0
Second band	0.9998	0.000013	0.0226	0.9992	0.000029	0.0528
Third band	0.9991	0.000052	0.0939	0.9967	0.000119	0.2167
Fourth band	0.9818	0.000707	1.2666	0.9541	0.000974	1.7441
Fifth band	0.0185	0.001863	3.3153	0	0	0
Sixth band	0.0009	0.000132	0.2350	0	0	0
Sum	4	0.002767	4.9333	3.95	0.001122	2.0134

structure of all compounds considered here. The calculated values for $n(E_F)$ can be obtained from Table III given below.

For the theoretical investigation of the Knight shift it is helpful to analyze the charge distribution. For this reason the charges inside touching atomic spheres are calculated. For the $B32$-type compound AB the volumes of the atomic spheres ω_A and ω_B have to coincide if the spheres touch each other. We have determined the partial density of states

$$q_y(E)=n(E)\int_{\omega_y}\rho_E(\mathbf{r})d\tau,\quad y=A,B\ , \tag{1}$$

where $\rho_E(\mathbf{r})$ is the electron density associated with the energy eigenvalue E. Then the total amount of charge inside the spheres is given by

$$Q_y=\int_{E_0}^{E_F} q_y(E)dE\ . \tag{2}$$

Inside the atomic spheres the wave functions are expanded in spherical harmonics.[6] From this expression the partial values for q_y and Q_y, associated with angular momentum l, $q_y^{(l)}$, and $Q_y^{(l)}$, have also been determined.

The partial densities of states $q_y(E)$ are plotted for NaIn in Fig. 1. For the first two bands $q_{\mathrm{Na}}(E)$ is much smaller than $q_{\mathrm{In}}(E)$. This is found for all Zintl phases AB. The first two bands are thus predominantly covalent bands formed by the diamondlike B sublattices.[7]

Table II shows the values for Q_y and $q_y(E_F)$ and the percentage s and p contribution of the sum of all valence states and of the electron states at the Fermi surface. Firstly, the $B^{\mathrm{III}a}$ elements in the $A^{\mathrm{I}a}B^{\mathrm{III}a}$ compounds shall be considered. Taking the mean over all valence states, the wave functions inside the $B^{\mathrm{III}a}$ spheres have approximately 50% s and 50% p character. For the stoichiometric phases these overall relations between s and p character do not differ drastically for the composition of the states at the Fermi surface, although a distinct d contribution of about 15% for states at the Fermi surface is calculated. For the defect phases, on the other hand, the percentage s character for states at the Fermi surface is much smaller than for the sum over the total number of occupied valence states. For the defect phases the fifth and sixth bands are empty and the Fermi surface is built exclusively from the second to fourth bands, which have a small s character at $E=E_F$.

The sensitivity of the s to p ratio on the position of the Fermi energy is even more pronounced for the A elements in $A^{\mathrm{I}a}B^{\mathrm{III}a}$. Firstly, the total amount of charge of the states with $E=E_F$ inside the A-type spheres is distinctly smaller for the defect (de) phases than for the stoichiometric (st) ones. That is, the electron states have significantly smaller amplitude in the A-type sublattice than in the $B^{\mathrm{III}a}$-type sublattice. For example, for LiAl, $q_{\mathrm{Li}}(\mathrm{st})=1.35$ and $q_{\mathrm{Al}}(\mathrm{st})=2.00$, whereas $q_{\mathrm{Li}}(\mathrm{de})=0.27$ and $q_{\mathrm{Al}}(\mathrm{de})=1.23$, see Table II. Secondly, for the A-type atoms of the defect phases the s components of the wave functions of the electronic states at the Fermi level are extremely small. In the defect phase LiAl, for example, the percentage of this s character for Li is only 4% compared with 64% for stoichiometric LiAl.

For the $A^{\mathrm{I}a}B^{\mathrm{II}b}$ phases LiZn and LiCd, the percentage of the s character for the A and $B^{\mathrm{II}b}$ atoms is smaller for the states at the Fermi surface than for the total number of states. This behavior is expected because, for s-p intermetallic phases, usually the p character increases with increasing energy.

TABLE II. Charge analysis of the electronic valence states of intermetallic Zintl compounds AB. All values are given in atomic units. Q_y, $y=A$ and B, are the total charges inside the atomic volumes and $q_y(E_F)$ are means of the partial densities of states at the Fermi surface. The percentages of l-partial charges, $l=s$ and p, $Q_y^{(l)}/Q_y$ and $q_y^{(l)}(E_F)/q_y(E_F)$ are also listed. For the $A^{\mathrm{I}a}B^{\mathrm{III}a}$ compounds the values are given for the stoichiometric (st) and the defect (de) phases.

		Q_y		$q_y(E_F)$		$Q_y^{(s)}/Q_y$		$q_y^{(s)}(E_F)/q_y(E_F)$		$Q_y^{(p)}/Q_y$		$q_y^{(p)}(E_F)/q_y(E_F)$	
AB		st	de	st	de	st	de	st	de	st	de	st	de
LiAl	Li	0.72	0.70	1.35	0.27	0.33	0.34	0.64	0.04	0.59	0.58	0.20	0.59
	Al	1.95	1.92	2.00	1.23	0.42	0.45	0.31	0.09	0.51	0.51	0.44	0.81
LiGa	Li	0.59	0.58	0.80	0.21	0.32	0.32	0.64	0.05	0.58	0.59	0.25	0.63
	Ga	1.97	1.95	1.38	0.89	0.51	0.51	0.44	0.11	0.47	0.46	0.41	0.82
LiIn	Li	0.66	0.65	1.51	0.26	0.34	0.34	0.65	0.01	0.56	0.57	0.24	0.63
	In	1.92	1.90	1.94	0.92	0.51	0.52	0.42	0.12	0.45	0.45	0.41	0.81
NaIn	Na	0.46	0.45	0.98	0.38	0.46	0.46	0.60	0.12	0.42	0.42	0.21	0.49
	In	2.04	2.01	2.24	1.90	0.55	0.56	0.20	0.07	0.42	0.42	0.70	0.88
LiZn	Li	0.49		1.98		0.38		0.20		0.55		0.72	
	Zn	1.38		3.61		0.59		0.13		0.38		0.82	
LiCd	Li	0.64		2.46		0.38		0.19		0.55		0.72	
	Cd	1.35		3.52		0.54		0.14		0.38		0.76	

TABLE III. Spin susceptibility $\chi^{(\hat{s})}$ for $B32$-type compounds AB in cgs volume units. For the $A^{\mathrm{I}a}B^{\mathrm{III}a}$ compounds the results are listed for the stoichiometric (st) and for the defect (de) phases. $\chi^{(\hat{s})}_{\mathrm{Pauli}}$ is the Pauli susceptibility deduced from the density of states; $\chi^{(\hat{s})}$ is the spin susceptibility including the exchange enhancement, and $\chi^{(\hat{s})}_{\mathrm{mol}}$ is the molar spin susceptibility in units of cm^3/mol.

		$\chi^{(\hat{s})}_{\mathrm{Pauli}}\times 10^6$	$\chi^{(\hat{s})}\times 10^6$	$\chi^{(\hat{s})}_{\mathrm{mol}}\times 10^6$
LiAl	st	0.61	0.68	13
	de	0.25	0.28	5
LiGa	st	0.45	0.48	9
	de	0.25	0.24	4
LiIn	st	0.53	0.59	14
	de	0.19	0.21	5
NaIn	st	0.45	0.48	14
	de	0.22	0.24	7
LiZn		1.25	1.60	29
LiCd		1.00	1.26	28

B. Susceptibility

In Table III the results for the calculated spin susceptibilities are listed. For the $A^{\mathrm{I}a}B^{\mathrm{III}a}$ compounds the data are given for the stoichiometric and the defect phases, see Secs. I and II A. The values $\chi^{(\hat{s})}_{\mathrm{Pauli}}$ are gained from the density of states using the Pauli expression,[6,13] whereas $\chi^{(\hat{s})}$ is calculated from the difference in the number of spin-up and spin-down electrons.[6] The difference between $\chi^{(\hat{s})}_{\mathrm{Pauli}}$ and $\chi^{(\hat{s})}$ is caused by the exchange enhancement effect.[14] For the alkali metals Li and Na, the exchange enhancement factor $f_{\mathrm{ex}}=\chi^{(\hat{s})}/\chi^{(\hat{s})}_{\mathrm{Pauli}}$ is known from experimental as well as theoretical investigations. One finds[15,16] $f_{\mathrm{ex}}(\mathrm{Li})=2.5$ and $f_{\mathrm{ex}}(\mathrm{Na})=1.6$. Minimizing the total energy within the spin-unrestricted procedure used here, including a magnetic energy of ±0.5 mRy (Ref. 6), one gets $f_{\mathrm{ex}}(\mathrm{Li})=2.01$ and $f_{\mathrm{ex}}(\mathrm{Na})=1.57$. These results give some assurance that, studying the spin susceptibility in Zintl phases, the calculated values $\chi^{(\hat{s})}$ are physically more correct than the data $\chi^{(\hat{s})}_{\mathrm{Pauli}}$.

Considering the values for $\chi^{(\hat{s})}$ given in Table III it can be seen that the smallest values $\chi^{(\hat{s})}$ are found for the $A^{\mathrm{I}a}B^{\mathrm{III}a}$ defect phases. The values $\chi^{(\hat{s})}[A^{\mathrm{I}a}B^{\mathrm{III}a}(\mathrm{st})]$ are larger by a factor of 2–3 than $\chi^{(\hat{s})}[A^{\mathrm{I}a}B^{\mathrm{III}a}(\mathrm{de})]$. The largest values for $\chi^{(\hat{s})}$ are found for the $A^{\mathrm{I}a}B^{\mathrm{II}b}$ compounds. These values are by a factor of 4 larger than $\chi^{(\hat{s})}[A^{\mathrm{I}a}B^{\mathrm{III}a}(\mathrm{de})]$. These differences in $\chi^{(\hat{s})}$ for the different Zintl phases are expected from the differences in the position of the Fermi energy considered in the preceding Sec. II A.

For the $A^{\mathrm{I}a}B^{\mathrm{II}b}$ compounds our results for the Pauli spin susceptibility $\chi^{(\hat{s})}_{\mathrm{Pauli}}$ agree satisfactorily with the values of Asada *et al.*[5] who found $\chi^{(\hat{s})}_{\mathrm{Pauli}}(\mathrm{LiZn})=1.08\times 10^{-6}$ and $\chi^{(\hat{s})}_{\mathrm{Pauli}}(\mathrm{LiCd})=0.95\times 10^{-6}$. For LiAl the results of Asada *et al.*[5] [$\chi^{\hat{s}}_{\mathrm{Pauli}}(\mathrm{LiAl,de})=0.37\times 10^{6}$, $\chi^{\hat{s}}_{\mathrm{Pauli}}(\mathrm{LiAl,st})=0.92\times 10^{-6}$] exceed our results noticeably. These discrepancies might be caused by differences in the band-structure results which are discussed below.

In Table IV the experimental values for the susceptibility χ_{expt} are listed. For a comparison of the measured and theoretical results the following experimental findings seem to be important: (a) χ_{expt} depends sensitively on the alkali concentration, (b) there are large differences in the results of Yao[11] and those of Klemm and Fricke,[17] (c) $\chi_{\mathrm{expt}}(\mathrm{LiCd})$ is temperature dependent, and (d) $\chi_{\mathrm{expt}}(\mathrm{NaIn})$ is not very well known. In the last two columns of Table IV the contributions of the valence electrons gained from χ_{expt} are shown. Our results for $\chi^{\mathrm{val}}_{\mathrm{expt}}$ differ from those of Yao[11] and those of Klemm and Fricke[17] because of differences in the used core wave functions. Our results for χ_{core} are based on $\langle r^2\rangle$ values gained from the density-functional approach. For the atoms considered here these $\langle r^2\rangle$ elements are about 5% larger than the ones obtained from Hartree-Fock wave functions.

The difference between $\chi^{(\hat{s})}_{\mathrm{mol}}$, Table III, and $\chi^{\mathrm{val}}_{\mathrm{expt}}$, Table IV, should yield some information about the orbital contribution $\chi^{(l)}\approx\chi^{\mathrm{val}}_{\mathrm{expt}}-\chi^{(\hat{s})}$. The comparison between $\chi^{\mathrm{val}}_{\mathrm{expt}}$

TABLE IV. Experimental values for the molar susceptibility in binary $B32$-type compounds in units of 10^{-6} cm^3/mol. The first two columns are the values of Klemm and Fricke, Ref. 17. These are average values of 48 to 52 at. % of Li. The third column contains the values of Yao, Ref. 11. These are interpolated values for the composition of 50 at. % Li. The fourth column contains the contribution of the core electrons gained for density-functional calculations for free atoms. In the fifth and sixth columns the contributions of the valence electrons are listed: $\chi^{\mathrm{val}}_{\mathrm{expt}\ 1}=\chi_{\mathrm{expt}\ 1}-\chi_{\mathrm{core}}$ and $\chi^{\mathrm{val}}_{\mathrm{expt}\ 3}=\chi_{\mathrm{expt}\ 3}-\chi_{\mathrm{core}}$. (Numbers in parentheses indicate error margins.)

	$\chi_{\mathrm{expt}\ 1}$ (90 K)	$\chi_{\mathrm{expt}\ 2}$ (293 K)	$\chi_{\mathrm{expt}\ 3}$ (293 K)	χ_{core}	$\chi^{\mathrm{val}}_{\mathrm{expt}\ 1}$	$\chi^{\mathrm{val}}_{\mathrm{expt}\ 3}$
LiAl	7	7	2	−4	11	6
LiGa			−13	−11		−2
LiIn	2(1)	2	−29	−22	24	−7
NaIn	−28(14)	−28		−27	−1(14)	
LiZn	4(1)	3	15	−13	17	28
LiCd	−11(1)	−2	7	−25	13	32

TABLE V. Bandwise contributions to the Knight shift $K_s^{(\hat{s})}$ (in %) for LiAl. $K_{s,n}^{\rm dir}$ is the direct spin contribution of the nth band and $K_{s,n}^{(\hat{s})}$ is the total spin term of the nth band. The values are listed for the stoichiometric (st) as well as for the defect (de) phases.

Band	$K_{s,n}^{\rm dir}$				$K_{s,n}^{(\hat{s})}$			
	st		de		st		de	
n	Li	Al	Li	Al	Li	Al	Li	Al
1	0	0	0	0	0.0001	−0.0031	0.0001	−0.0031
2	0.0000	0.0001	0.0001	0.0003	0.0001	−0.0049	0.0001	−0.0045
3	0.0000	0.0000	0.0000	0.0000	0.0000	0.0001	0.0001	0.0002
4	0.0001	0.0078	0.0002	0.0166	0.0001	0.0105	0.0003	0.0172
5	0.0170	0.0780	0	0	0.0185	0.0838		
6	0.0013	0.0057	0	0	0.0013	0.0059		
Sum:	0.0184	0.0916	0.0003	0.0169	0.0201	0.0923	0.0006	0.0098

and $\chi^{(\hat{s})}$ shows that for the $A^{\rm Ia}B^{\rm IIIa}$ compounds, $\chi^{(\hat{s})}$ and $\chi^{(\hat{l})}$ should be in the same order of magnitude. For the $A^{\rm Ia}B^{\rm IIb}$ compounds it might be possible that $\chi^{(\hat{s})}$ dominates. An accurate calculation of the orbital contribution $\chi^{(\hat{l})}$ is extremely complicated[18–20] and could not be performed in the present work.

C. Knight shift

In this section the calculated spin contributions to the Knight shift, $K_s^{(\hat{s})}$, are presented. The total $K_s^{(\hat{s})}$ deduced from the spin-polarized procedure[6] can be separated into three contributions. According to the Pauli paramagnetism one gets a Fermi contact term $K_s^{\rm dir}$ of the singly occupied electronic states $\psi_{\mathbf{k}_F}$ at the Fermi surface. This direct interaction[21]

$$K_s^{\rm dir}=\frac{8\pi}{3}\chi_{\rm Pauli}^{\hat{s}}\langle\,|\psi_{\mathbf{k}_F}(0)|^2\rangle_{F\omega} \qquad (3)$$

has to be corrected due to the exchange enhancement of the susceptibility,[14,22] see above. Additionally, the doubly occupied electronic states below the Fermi surface produce a hyperfine field at the nuclei due to the exchange polarization effect.[6,23,24] In Table V, $K_s^{\rm dir}$ and the total spin term $K_s^{(\hat{s})}$ are given bandwise for LiAl. In Table VI, $K_s^{\rm dir}$ and $K_s^{(\hat{s})}$ are listed for all compounds considered here. The first band is fully occupied (see Table I) and therefore the term $K_{s,1}^{(\hat{s})}$ is a pure exchange polarization contribution. To demonstrate, the size of the exchange polarization term $K_{s,1}^{(\hat{s})}$ is displayed in Table VI.

The values for $K_s^{(\hat{s})}$ are closely correlated to the partial s charges considered above (Table II) because only the s

TABLE VI. Knight shift (in %) for intermetallic Zintl compounds AB. $K_{s,1}^{(\hat{s})}$ are the contributions of the first valence bands due to the exchange polarization effect; $K_s^{\rm dir}$ are the direct spin terms, Eq. (3); $K_s^{(\hat{s})}$ are the total spin results; and $K_s^{\rm expt}$ are the experimental data. For comparison, K_s for the pure metals are given too. For the $A^{\rm Ia}B^{\rm IIIa}$ compounds the theoretical results are listed for the stoichiometric (st) as well as for the defect (de) phases. (Numbers in parentheses denote error margins.)

AB		$K_{s,1}^{(\hat{s})}$	$K_s^{\rm dir}$		$K_s^{(\hat{s})}$		$K_s^{\rm expt}$ (Ref. 25)	K_s in the pure metals (Ref. 25)
			st	de	st	de		
Li-Al	Li	0.0001	0.018	0.0003	0.020	0.001	<0.005	0.026
	Al	−0.003	0.09	0.02	0.09	0.01	0.010(3)	0.164
Li-Ga	Li	0.0001	0.012	0.0005	0.015	0.001	<0.005	0.026
	Ga	−0.007	0.28	0.05	0.25	0.04	0.09(1)	0.146
Li-In	Li	0.0001	0.018	0.0004	0.022	0.001	<0.005	0.026
	In	−0.025	0.63	0.09	0.58	0.06	0.13(2)	0.82
Na-In	Na	0.0002	0.038	0.003	0.050	0.003		0.113
	In	−0.024	0.33	0.10	0.30	0.08	0.07;0.22	0.82
Li-Zn	Li	0.0003	0.010		0.013		0.00(1)	0.026
	Zn	−0.035	0.18		0.15		0.20(5)	0.20
Li-Cd	Li	0.0004	0.010		0.012		0.01	0.026
	Cd	−0.078	0.32		0.25		0.39(2)	0.415

part of a wave function has a finite density at the nucleus. Therefore, the same trends as shown for $q_y^{(s)}(E_F)$ in Sec. II A are also found for $K_s^{(\hat{s})}$.

From Table V it can be seen that the largest direct contributions to $K_s^{(\hat{s})}$ for stoichiometric LiAl are due to the fifth band, which has a large s component at the bottom of the band. From this term large values for $K_s(\underline{\mathrm{Li}}\mathrm{Al})$ and $K_s(\mathrm{Li}\underline{\mathrm{Al}})$ result, which are not found experimentally, see Table VI. The same holds for all $A^{\mathrm{I}a}B^{\mathrm{III}a}$ compounds. For the defect phases, however, the resulting theoretical values $K_s^{(s)}$ are close to the experimental data K_s^{expt}. For the $A^{\mathrm{I}a}B^{\mathrm{III}a}$ compounds K_s is very small, because both the density of states at the Fermi surface (Table III) and the s amplitudes of the wave functions of the states at the Fermi surface (Table II) are small. This behavior explains why the values $K_s(A^{\mathrm{I}a}B^{\mathrm{III}a})$ are much smaller than those found experimentally for the pure metals (see last column of Table VI). The drastic differences between the spectroscopic data for the ideal and defect $A^{\mathrm{I}a}B^{\mathrm{III}a}$ compounds can also be seen from the values of $r = \langle \, | \psi_{\mathbf{k}_F}(0) |^2 \rangle_{F\omega}$ (r is equal to 1 within the free electron model). r can be calculated from Eq. (3) using K_s^{dir}, Table VI, and $\chi_{\mathrm{Pauli}}^{(\hat{s})}$, Table III. One finds for the In nuclei sites in the ideal phase LiIn, $r = 1418$, whereas for the defect phase the mean of the s amplitude is reduced by a factor of 10, $r = 113$.

For the $A^{\mathrm{I}a}B^{\mathrm{II}b}$ compounds the charge distributions at the Fermi surface show the normal l dependence of s-p metals. It follows that one finds for the $A^{\mathrm{I}a}B^{\mathrm{II}b}$ alloys experimentally and theoretically large paramagnetic Knight shifts, which are close to K_s of the pure metals, see Table VI.

It is surprising that the theoretical values for $K_s(A\underline{B})$, deduced from the spin-polarized procedure, $K_s^{(\hat{s})}$, are smaller than the direct contribution of the states at the Fermi surface, K_s^{dir}, in spite of the fact that $K_s^{(\hat{s})}$ contains the exchange enhancement. Within the procedure used here, however, the exchange enhancement effect is smaller in size than a negative exchange polarization of the first two valence bands of the B sublattice. The order of magnitude of the negative exchange polarization can be seen from the contribution $K_{s,1}^{(\hat{s})}$, see above.

Finally in this section our results for the direct contributions to K_s,K_s^{dir} shall be compared with the data calculated by Asada *et al.*[5] These authors found $K_s(\mathrm{Li}\underline{\mathrm{Al}},\mathrm{st}) = 0.169\%$, $K_s(\mathrm{Li}\underline{\mathrm{Al}},\mathrm{de}) = 0.027\%$, $K_s(\mathrm{Li}\underline{\mathrm{Zn}}) = 0.16\%$, and $K_s(\mathrm{Li}\underline{\mathrm{Cd}}) = 0.20\%$. For LiAl these values are by about a factor of 2 larger than our results, whereas for the $A^{\mathrm{I}a}B^{\mathrm{II}b}$ compounds our results are larger than those of Asada *et al.* The differences in K_s^{dir} between our results and those of Asada *et al.* show the same trends as the calculated values $\chi_{\mathrm{Pauli}}^{(\hat{s})}$ considered above. The percentage differences, however, are remarkably larger for K_s^{dir} than for $\chi_{\mathrm{Pauli}}^{(\hat{s})}$. It follows that both the densities of states and the s partial densities differ. This will be discussed below.

III. DISCUSSION

A. Band structure

In this section differences in the band structure of LiAl obtained by different methods shall be described. Table VII shows the energy separation for various levels of LiAl gained by different authors. Our results are calculated from the self-consistent scalar relativistic augmented-plane-wave method with the exchange correlation potential proposed by Vosko *et al.*[26] Asada *et al.*[5] used the nonrelativistic linear-muffin-tin-orbital method within the atomic-sphere approximation with the exchange-correlation potential of Hedin and Lundqvist,[27] and the data of Zunger[4] are deduced from the discrete variational energy-band method. Comparing the data given in Table VII one sees that there is no unique trend for all energy separations ΔE. This indicates that the differences in the ΔE values are caused by differences in the hybridization of the Li and Al valence orbitals as the position of the levels depend on the basis functions used for the calculation. This is most obvious for the electronic states at the Fermi surface. In the LCAO methods the wave functions inside the Li atomic spheres are expanded in s and p functions. In the augmented-plane-wave procedure, on the other hand, the wave functions of the electronic states at the Fermi level inside the Li spheres have 80% s and p amplitudes (see Table II) and 20% d character. We think that for LiAl and LiZn the influence of the different basis sets is responsible for the differences in the calculated direct contributions to χ and K_s considered in the preceding section. For LiCd also relativistic effects might be important.

TABLE VII. Comparison of energy separation (in Ry) for various levels in LiAl with those of Zunger (Ref. 4) and Asada *et al.* (Ref. 5).

	Present	Asada *et al.*	Zunger
Valence-valence			
$X_1 \rightarrow X_4$	0.233	0.223	0.217
$X_{2'} \rightarrow L_1$	0.146	0.136	0.150
$L_1 \rightarrow L_{3'}$	0.341	0.367	0.339
Valence-exited			
$\Gamma_1 \rightarrow \Gamma_{25'}$	0.682	0.702	0.694
$X_4 \rightarrow X_1$	0.191	0.193	0.256
$L_{3'} \rightarrow L_3$	0.085	0.051	0.110
$X_1 \rightarrow \Gamma_{25'}$	0.040	0.062	0.013

B. Knight shift

First, differences in the calculated values for the Knight shift $K_s^{(\hat{s})}$ for the stoichiometric (st) phases $A^{\mathrm{I}a}B^{\mathrm{III}a}$ with $N_{VE} = 4$ and the defect (de) phases with $N_{VE} < 4$ shall be considered. As pointed out in Sec. II C one finds that the data $K_s^{(\hat{s})}(A^{\mathrm{I}a}B^{\mathrm{III}a},\mathrm{st})$ are much larger than $K_s^{\mathrm{expt}}(A^{\mathrm{I}a}B^{\mathrm{III}a})$. This discrepancy is caused by the large hyperfine fields produced by the singly occupied electronic states of the fifth and sixth valence bands. These electronic states are nonoccupied for phases with defects V_A and A_B for which $K_s^{(\hat{s})}$ and K_s^{expt} agree satisfactorily, see Table VI. For a more quantitative comparison between K_s^{theor} and K_s^{expt} one has to know the exact number of defects and additionally the orbital contribution $K_s^{(\hat{l})}$.

First we want to make some remarks on $K_s^{(\hat{l})}$. In a rough approximation $K_s^{(\hat{l})}$ can be separated into a long-range term and two short-range contributions.[28-33] Estimating the long-range diamagnetic shielding by the free-electron result[28] and the short-range diamagnetic contribution by the Lamb expression,[29,30] one gets for the AB phases considered here, total diamagnetic shieldings for the nonalkali nuclei less than -0.002×10^{-2}; that is, the diamagnetic orbital contributions to the Knight shift seem to be small compared to $K_s^{(\hat{s})}$.

The paramagnetic orbital contribution K_s^{orb}, however, seems to be more important.[5] In a simple approach K_s^{orb} is given by[9,31]

$$K_s^{\text{orb}}=\frac{8\pi}{3}\chi^{\text{orb}}\langle r^{-3}\rangle\omega_{\text{WS}}\ , \tag{4}$$

where χ^{orb} is the local (van Vleck) orbital susceptibility of the atom considered, ω_{WS} is the Wigner-Seitz volume for this atom, and $\langle r^{-3}\rangle$ is the expectation value of r^{-3}.

From the results for $\chi^{(\hat{s})}$ and χ^{expt}, Tables III and IV, one can conclude that χ^{orb} should be in the range of $\chi^{\text{orb}}\approx0.2\times10^{-6}$. Calculating $\langle r^{-3}\rangle$ for an outermost atomic p function one gets $\langle r^{-3}\rangle_{\text{Al},3p}\approx 1a_0^{-3}$ and $\langle r^{-3}\rangle_{\text{In},5p}\approx 5a_0^{-3}$. Then using Eq. (4), one gets an estimate of the paramagnetic orbital contribution of $K_s^{\text{orb}}(A\underline{B})\approx0.03\times10^{-2}$ increasing with increasing atomic number of the B element.

Besides the contribution $K_s^{(\hat{l})}$ to K_s^{expt} the influence of the number of defects on the Knight shift shall be considered. Figure 2 shows the calculated spin contribution $K_s^{(\hat{s})}$(LiIn) as a function of N_{VE}. It can be seen that $K_s^{(\hat{s})}$ depends sensitively on N_{VE}. Assuming a net paramagnetic orbital Knight shift, $K_s^{(\hat{s})}$ should be smaller than K_s^{expt}. On the basis of this assumption, agreement between K_s^{theor} and K_s^{expt} can only be found for $3.92\lesssim N_{VE}\lesssim3.96$, see Fig. 2. Calculating the Li-NMR shift in LiIn ($K_s^{\text{expt}}<0.005\%$) within the rigid-band model, one gets $K_s^{(\hat{s})}<0.005\%$ for $N_{VE}<3.96$. Analogously, one finds for the LiAl and LiGa defect phases $3.92\lesssim N_{VE}\lesssim3.98$ and $3.89\lesssim N_{VE}\lesssim3.98$, respectively. For LiAl the lower limit of this range ($N_{VE}\approx3.92$) coincides with the values deduced from density measurements.[12] If one assumes that (i) the alloys are prepared from 50% Li and 50% $B^{\text{III}a}$ and (ii) the defect mechanisms are vacancies in the Li lattice (V_{Li}) and substitutionals in the B lattice (Li_B) (Ref. 12), the concentration of the B atoms in the B sublattice is equal to

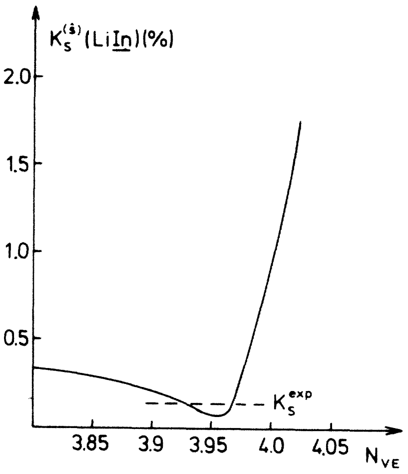

FIG. 2. Calculated spin contribution to the Knight shift at the In nuclei in Li-In $K_s^{(\hat{s})}$ (Li$\underline{In}$) as a function of the number of valence electrons N_{VE} per half unit cell. The experimental value K_s^{expt} is shown too.

$$B_B=\frac{N_{VE}-1}{3}\ . \tag{5}$$

Within this picture one can conclude from our theoretical studies that the number of substitutionals in the $B^{\text{III}a}$ sublattice is more than 0.5% and less than 3.5%.

In summary, two conclusions can be drawn from the theoretical investigations of K_s. Firstly, one finds that the spin contributions and the paramagnetic orbital contribution seem to be predominant terms for K_s. The small chemical shifts in the $A^{\text{I}a}B^{\text{III}a}$ compounds can be explained by small densities of states at the Fermi surface and by small s amplitudes of the electron states at the Fermi surface. The exchange enhancement effect is smaller than a negative exchange polarization of inner valence states. Secondly, for all $A^{\text{I}a}B^{\text{III}a}$ compounds, agreement between K_s^{expt} and K_s^{theor} can only be found for phases for which the number of valence electrons per half unit cell is less than 4. This finding supports the assumption[12] that the defect structure found for LiAl (Ref. 12) (vacancies V_A in the alkali sublattice and substitutionals A_B in the nonalkali sublattice) is present in all $B32$-type $A^{\text{I}a}B^{\text{III}a}$ compounds.

ACKNOWLEDGMENTS

The author thanks Professor Dr. Alarich Weiss for continuous support and interest in the present work and Dr. M. C. Böhm and Dr. P. Bopp for helpful discussions.

---

[1] E. Zintl, Angew. Chem. **52**, 1 (1939).

[2] P. W. Anderson, *Concepts in Solids* (Benjamin, New York, 1963), p. 6; L. Brewer, in *High Strength Materials,* edited by V. Zackay (Wiley, New York, 1964), p. 37; N. Engel, in *Developments in the Structural Chemistry of Alloy Phases,* edited by B. Giessen, (Plenum, New York, 1969), pp. 25—40; W. Hückel, *Structural Chemistry of Inorganic Compounds* (Elsevier, Amsterdam, 1951), p. 829 ff.

[3] J. Robertson, Solid State Commun. **47**, 899 (1983).

[4] A. Zunger, Phys. Rev. B **17**, 2582 (1978).

[5] T. Asada, T. Jarlborg, and A. J. Freeman, Phys. Rev. B **24**, 510 (1981); **24**, 857 (1981).

[6] P. C. Schmidt, Phys. Rev. B **31**, 5015 (1985).

[7] P. C. Schmidt, Z. Naturforsch. **40A**, 335 (1985).

[8] N. E. Christensen, Phys. Rev. B **32**, 207 (1985).

[9] R. E. Watson, L. H. Bennett, G. C. Carter, and I. D. Weisman, Phys. Rev. B **3**, 222 (1971).

[10] W. Klemm, Proc. Chem. Soc. London (1958), p. 329.

[11] Y. L. Yao, Trans. Soc. Metall. AIME **230**, 1725 (1964).

[12] H. E. Schone and W. D. Knight, Acta Metall. **11**, 179 (1963); K. Kishio and J. O. Brittain, J. Phys. Chem. Solids **40**, 933 (1979).

[13] W. Pauli, Z. Phys. **41**, 81 (1927).

[14] S. D. Silverstein, Phys. Rev. **130**, 912 (1963); A. Narath and H. Weaver, Phys. Rev. **175**, 373 (1968); S. D. Mahanti and T. P. Das, Phys. Rev. B **3**, 1599 (1971).

[15] T. Kushida, J. C. Murphy, and M. Hanabusa, Phys. Rev. B **13**, 5136 (1976).

[16] A. H. MacDonald, K. L. Liu, S. H. Vosko, and L. Wilk, Can. J. Phys. **59**, 500 (1981).

[17] W. Klemm and H. Fricke, Z. Anorg. Allg. Chem. **282**, 162 (1955).

[18] J. E. Hebborn and E. H. Sondheimer, J. Phys. Chem. Solids **13**, 105 (1960).

[19] L. M. Roth, J. Phys. Chem. Solids **23**, 433 (1962).

[20] E. I. Blount, Phys. Rev. **126**, 1636 (1962).

[21] W. D. Knight, Solid State Phys. **2**, 93 (1956).

[22] A. M. Clogston and V. Jaccarino, Phys. Rev. **121**, 1357 (1961).

[23] M. H. Cohen, D. A. Goodings, and V. Heine, Proc. Phys. Soc., London **73**, 811 (1959).

[24] G. D. Gaspari, W. M. Shyu, and T. D. Das, Phys. Rev. **134**, A852 (1964).

[25] G. C. Carter, L. H. Bennett, and D. J. Kahan, in *Metallic Shifts in NMR*, Vol. 20 of *Progress in Material Science*, edited by B. Chalmers, J. W. Christian, and T. B. Massalski (Pergamon, New York, 1977).

[26] S. H. Vosko, L. Wilk, and M. Nusair, Can. J. Phys. **58**, 1200 (1980).

[27] L. Hedin and B. I. Lundqvist, J. Phys. C **4**, 2064 (1971).

[28] T. P. Das and E. H. Sondheimer, Philos. Mag. **5**, 529 (1960).

[29] W. Lamb, Phys. Rev. **60**, 817 (1941).

[30] J. E. Hebborn, Proc. Phys. Soc. London **80**, 1237 (1962).

[31] Y. Yafet and V. Jaccarino, Phys. Rev. **133**, A1630 (1964); J. A. Switendick, A. C. Gossard, and V. Jaccarino, Phys. Rev. **136**, A1119 (1964).

[32] L. Landau, Z. Phys. **64**, 629 (1930).

[33] R. Peierls, Z. Phys. **80**, 763 (1933).